RSC Advances

PAPER

View Article Online
View Journal | View Issue

Cite this: *RSC Adv.*, 2015, **5**, 628

Tuning emission and Stokes shift of CdS quantum dots *via* copper and indium co-doping†

Mingming Liu,[ab] Wei Yao,[ac] Cun Li,[b] Zhenyu Wu[b] and Liang Li*[a]

Received 27th September 2014
Accepted 25th November 2014

DOI: 10.1039/c4ra11349g

www.rsc.org/advances

Strongly luminescent copper and indium co-doped CdS quantum dots (CuIn-doped CdS QDs) were synthesized from copper iodide, indium acetate, cadmium oleate, and 1-dodecanethiol as starting compounds in octadecene solvent. We demonstrated that when co-doping with In, Cu ions can homogeneously dope into CdS QDs and exist in the +1 state. The as-prepared doped QDs exhibited photoluminescence (PL) in the range of 590–800 nm, with a maximum fluorescence quantum yield (QY) of 40%. They also exhibited tunable large Stokes shifts from 100 nm to 300 nm *via* tuning dopant concentrations of Cu and In. Such an extremely large Stokes shift dramatically decreased the self-reabsorption of QDs. Furthermore, the CuIn-doped CdS QDs exhibited excellent thermal stability and lost only approximately 20% of their emission QY when the temperature was increased from 20 °C to 150 °C. These features make these QDs suitable as emitters for application in lighting.

Introduction

Semiconductor nanocrystals, *i.e.*, quantum dots (QDs), have attracted substantial attention in the lighting and display industries because they offer many potential advantages as down-conversion phosphors.[1–6] For example, the emission spectra of QDs can be "tuned" by controlling their particle size and/or surface chemistry, unlike conventional phosphors, whose emission spectra are largely fixed by nature. Furthermore, QDs usually exhibit efficient (large absorption cross-sections) and broad absorption and can be easily excited by blue light-emitting diode (LED) chips. Compared with conventional micrometer-scale rare-earth phosphors, QDs as nanoscale phosphors offer some advantages, such as negligible back and internal scattering,[7] which are very beneficial in improving LED efficiency. These features have attracted extensive interest from both academic and industry researchers, and QDs have recently been demonstrated to function as color-converting phosphors in single-color, white-light-emitting devices and in displays.[8–13] However, as with some conventional phosphors, a key issue limiting QDs for down-conversion phosphor applications is the small Stokes shift (*i.e.*, the spectral separation between absorption onset and emission) characteristic of these nanomaterials, which results in strong self-reabsorption (or yellow/green absorption by red-emitting QDs). This reabsorption is anticipated to limit the solid-state efficiencies of these QDs when their packing density or loading fraction is increased.[7,14,15]

Therefore, the synthesis of highly luminescent QDs with a large Stokes shift would be interesting from the perspective of their application as a down-conversion phosphor. Doped QDs provide a larger Stokes shift than do conventional QDs, where the hosts for doping maintain their own absorption features and the emission wavelength is primarily determined by the intra-gap states of the dopant ions.[16] Transition-metal ions such as Mn[17–20] and Cu[21–34] ions are often used as luminescent centers and have been demonstrated to be efficient emitters that cover the blue-to-red color window. However, the synthesis of Mn- or Cu-doped QDs often requires very sophisticated synthetic chemistry to overcome the difficult incorporation of Mn and Cu ions into the host lattices. For example, a core/shell structure is usually used to avoid the exclusion of Cu ions (*i.e.*, lattice ejection)[32] from the host nanocrystals during the synthesis of Cu-doped QDs, such as Cu:ZnS/ZnCdS,[35] Cu:ZnSe/CdSe[36] or Cu:CdS/CdS.[37] In these systems, doped QDs are obtained by first synthesizing undoped QDs at high temperatures, cooling them for the addition of a Cu precursor, followed by applying an overcoating of a shell of the same or another semiconductor material, where the dopant ions are first adsorbed onto the surface of seed QDs and then buried by the overcoating of outside layers.[35–37]

[a]*School of Environmental Science and Engineering, Shanghai Jiao Tong University, Shanghai, China, 200240. E-mail: liangli117@sjtu.edu.cn*

[b]*School of Chemistry and Chemical Engineering, Anhui University, Hefei, China, 230601*

[c]*College of Chemistry and Chemical Engineering, Shanghai University of Engineering Science, Shanghai, China, 201620*

† Electronic supplementary information (ESI) available: PL evolution of CuIn-doped CdS with reaction time, comparison of PL and absorption spectra for the samples with different D-concentrations but a same absorption shoulder position, XPS overview spectra, the overlap of the emission and absorption spectra of CuIn-doped CdS, CdSe, CdSe/CdS, $CuInS_2$, and $CuInS_2$/ZnS QDs, and the evolution of the M/Cd molar ratio in dope CdS QDs with increasing reaction time (M = Cu, In). See DOI: 10.1039/c4ra11349g

Over the past several decades, indium, gallium or aluminum have often been used as an activator in the conventional synthesis of micrometer-scale Cu:ZnS phosphors.[38–42] These group-III elements not only behave as charge compensators to correct the charge imbalance caused by Cu doping but also enhance the solubility of Cu in the host, resulting in internally doped crystals. From this point of view, the doping of Cu in conjunction with In into CdS will be much easier than directly doping Cu alone into CdS. In this work, we used a similar strategy to co-dope Cu and In into CdS and surprisingly synthesized highly luminescent CuIn-doped CdS QDs, which exhibit a high QY and show tunable emission from the green-yellow to the near-infrared region (590–800 nm) with adjustable large Stokes shift (200–300 nm).

Results and discussion

Spectra characterizations of CuIn-doped CdS QDs

CuIn-doped CdS QDs were synthesized by a heating-up procedure using copper iodide, indium acetate, cadmium oleate, and 1-dodecanethiol as starting compounds and octadecene as a solvent. Different amounts of the Cu and In precursors were added with a fixed amount of Cd precursor to investigate the effects of dopant concentration (D-concentration). D-concentration is defined as the dopant/host (CuIn/CdS) atomic ratio of the precursors mixture in this paper if without special notes. The mixture was heated to 120 °C under a primary vacuum for 0.5 h, backfilled with N_2, and then heated to the reaction temperature of 250 °C at a rate of 13 °C min^{-1}. After the reaction solution was heated up to 250 °C, the color of samples with low dopant levels turned light-green and slowly changed to deep-green with increasing reaction time. This change is consistent with the absorption spectra, where the sharp absorption shoulders shift very slowly from 370 nm to 400 nm indicating the slow growth of the CdS QDs in the quantum confinement regime. Meanwhile, the emission of CdS QDs shifted from green to deep-red and even to the near-infrared with increasing reaction time (Fig. 1a). Such a large red shift is very similar to the observation in the synthesis of copper(I) doped CdS QDs.[33]

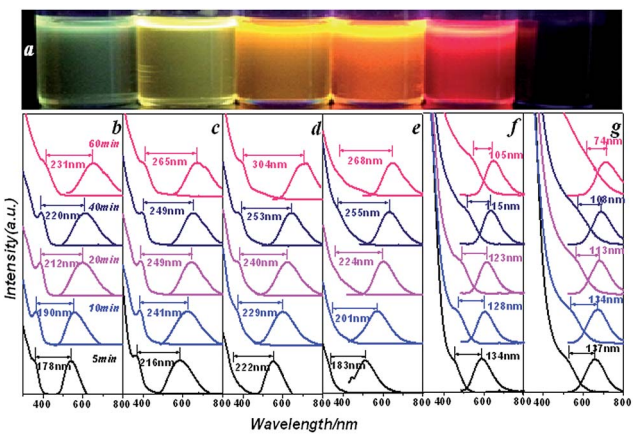

Fig. 1 (a) Digital pictures of the samples (D-concentration 10%) taken at different reaction times under a 365 nm UV lamp; evolutions of the absorption and PL spectra of samples with reaction time at different D-concentrations (b) 2.5%, (c) 6.5%, (d) 10%, (e) 20%, (f) 45%, (g) 100%).

However, this sharp absorption shoulder began to disappear with increasing D-concentration and almost disappeared when the D-concentration reached 20%. When the concentration of Cu and In was further increased to 45% (Fig. 1f), a broad shoulder again emerged; this shoulder is very similar to that in the spectrum of $CuInS_2$ QDs.[43–47] Absorption features usually represent the band structures of QDs. For samples with low concentrations of dopant, the absorption band is primarily determined by the nature of the CdS QDs, including their size and size distribution that was also observed in the single-doped system (Cu:ZnS,[33] Cu:CdZnS[35]), where the effects of dopant ions on the absorption are almost negligible and the absorption spectra are always sharp and shift with growth. However, when additional Cu and In ions were incorporated into the CdS lattice, the band structure changed and finally formed an absorption band of alloyed $Cu_xIn_xCd_{1-x}S_2$ with contributions from Cu and In, whose absorption spectra usually exhibit a shallow shoulder.[43]

As shown in Fig. 1b–f, all of the CuIn-doped CdS QDs exhibited a large Stokes shift. However, the evolution of the Stokes shift at lower D-concentrations differs substantially from that observed at the highest D-concentration (45%). At lower concentrations, the Stokes shift increased with increasing reaction time. For example, in the reaction with a D-concentration of 2.5%, the Stokes shifts of the QDs changed from 178 nm to 231 nm as the reaction time increased from 5 minutes to 60 minutes. A higher D-concentration of 10% led to even greater Stokes shifts compared with those of the samples synthesized with lower dopant levels. The largest Stokes shift of 304 nm was observed in the case of the sample synthesized for 60 minutes. However, a further increase in the concentration of Cu and In to 20% decreased the Stokes shift. When the Cu/Cd molar ratio of the precursors was 45% (Fig. 1f), the Stokes shift decreased to approximately 100 nm and shrinked with reaction time, which is similar to our observations in the synthesis of $CuInS_2$ QDs (Fig. 1g).

To clarify the luminescence mechanisms of CuIn-doped CdS at low and high D-concentrations, the PL (photoluminescence) dynamics of CuIn-doped CdS with different D-concentrations were investigated and the corresponding PL decay curves are shown in Fig. 2a. We observed that the PL decay in the low D-concentration (6.5%) QDs samples is not single-exponential decay and that the decay is faster on the emission band (τ = 91.4 ns) than on the another band (τ = 665.8 ns), as shown in the Fig. 2a inset. However, the fast channel is not observed in our high D-concentration (20%) samples, perhaps because the transition to alloy structure eliminates the fast radiative channel with increasing D-concentration. The current biexponential analysis indicates that the PL signal is associated with a higher-energy band and a lower-energy band with a long lifetime in the low D-concentration. At this stage, the origin of the biexponential dynamics is not fully understood; however, one possible explanation is an emissive transition involving an electron quantized state and a localized hole state.

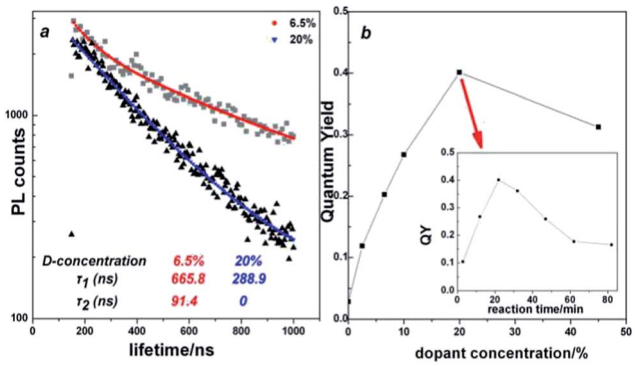

Fig. 2 (a) Time-resolved photoluminescence spectra of 6.5% and 20% CuIn-doped CdS QDs. (b) QYs of the samples synthesized with different D-concentrations but with a similar absorption shoulder position (the inset is the time evolution of the QYs of the samples with respect to the reaction time with D-concentration of 20%).

The QY of CuIn-doped CdS QDs was measured using a standard method for ref. 48. As shown in Fig. 2b, the QY of the CuIn-doped CdS QDs increased with increasing reaction time and reached its highest value at approximately 20 minutes; it thereafter decreased. We observed that the Cu and In doping concentration substantially affects the QYs of CuIn-doped CdS QDs, which increases with increasing D-concentration from 2.5% to 20%, but decreases a little at D-concentration of 45% for those samples with a similar absorption shoulder position. The result indicates that the luminescence mechanism of our system is quite different from that of rare-earth-doped phosphors, where high concentrations of doping ions quench luminescence.

A simple model is proposed schematically in Fig. 3 to explain the aforementioned spectral behaviors. We consider the samples with low Cu and In concentrations to be a doped system; however, we consider the sample with the highest Cu and In concentrations (45%) to be an alloy structure rather than a doped system. The recombination process of both cases can be considered two processes. In one process, a localized defect state captures a hole from the valence band; in the other process, the electron transfers from a quantized state (*i.e.*, the conduction band) to a hole-trapped defect state with radiative emission.[25,43] With increasing QD sizes, the quantized conduction band moves downward and the valence band moves upward. Because of the small effective mass of the electron compared to that of the hole,[35,49] the change in the conduction band structure with size growth is greater than the change in the valence band. However, the difference between the two cases is the evolution of a defect state position with the growth of the QDs. In the former system (Fig. 3c), the defect state may have moved upward with increasing size of the QDs, resulting in a more red emission and larger Stokes shifts compared with the latter system. In the alloyed structure of the latter system, the defect state position is most likely fixed at a constant level, which causes the Stokes shift to gradually shrink as the QDs grow, as shown in Fig. 3d. This hypothesis can well explain the aforementioned spectral features, including the larger Stokes shift and the increased red emission in the samples with lower D-concentrations. The previously discussed defects can originate from the different bonding nature of Cu–S and In–S or from typical defects such as a substitutional defect, in which group-I and group-III ions are swapped. Unfortunately, not much is thus far known about the exact nature of the defects in CuIn-doped QDs that are responsible for PL transitions.

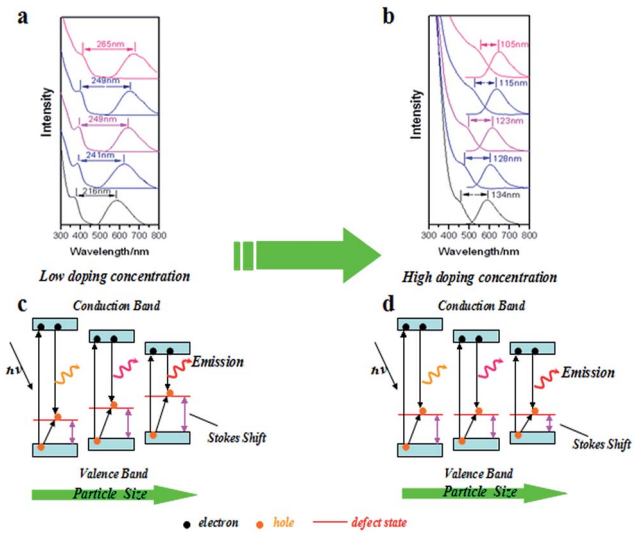

Fig. 3 Evolutions of the Stokes shifts in the spectra of CuIn-doped QDs' (a and b) with increasing reaction time for low and high D-concentrations and schematics of their corresponding mechanisms (c and d).

Structural characterizations

Fig. 4 is the typical transmission electron microscopy (TEM) images of CuIn-doped CdS QDs with a D-concentration of 10%; the images show that the sizes of the QDs sampled at 10 minutes and 30 minutes are 2.51 nm ± 0.38 nm and 2.75 nm ± 0.31 nm, respectively. The increasing size indicates that the CdS QDs grew during the synthesis process. The inset images are high-resolution TEM pictures of CuIn-doped CdS QDs. The lattice distance is almost identical to that of pure CdS, which we further confirmed by XRD characterizations. The XRD patterns of samples with different doping levels are shown in Fig. 5a. For comparison, the diffraction peaks of bulk CdS crystals are

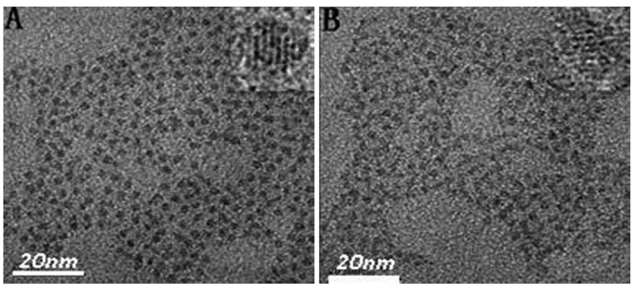

Fig. 4 TEM images of CuIn-doped CdS QDs (D-concentration 10%) synthesized at different reaction times (A: 10 min; B: 30 min).

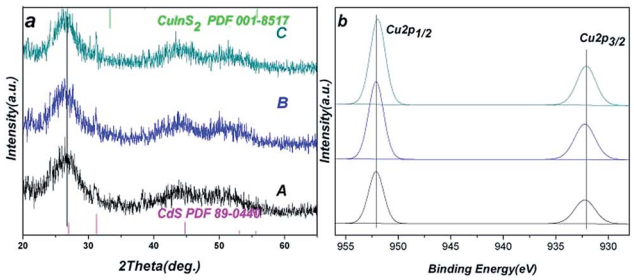

Fig. 5 (a) X-ray diffraction profiles and (b) Cu 2p XPS of CdS QDs with different D-concentrations (A 2.5%, B 10%, C 20%), recorded at an excitation energy of 1253.6 eV.

marked as solid lines in Fig. 5a. No obvious difference was observed between the patterns of the three samples.

The oxidation state of Cu ions in the doped semiconductor system, as an argument over the existence of Cu(I)[33,50] and Cu(II),[51–53] has long been a topic of debate, with support for both states being published in the literatures. To know the valence state of the Cu ions in our system, we performed X-ray photoelectron spectroscopy (XPS) analysis. Fig. 5b shows that the Cu $2p_{3/2}$ signal is centered at 952.4 eV, whereas the Cu $2p_{1/2}$ signal is located at 932.6 eV, which matches well with the 2p signals of Cu^{+} in previous reports[54,55] and is very different from the signals of Cu^{2+} $2p_{3/2}$ and $2p_{1/2}$ that centered at 933.6 eV and 953.6 eV, respectively.[56] These results suggest that Cu ions exist in +1 state in our system.

Two possible structures can induce such a large Stokes shift observed in our samples: the doping structure and a type-II core/shell structure such as $CuInS_2$/CdS, where the electrons are highly delocalized to the core and shell, resulting in a substantial red shift emission compared with that of the core QDs. We cannot discern from the XRD and TEM data whether our sample is a doped or core/shell structure. To clarify whether our samples are core/shell-structured, we performed an elemental analysis by ICP-OES (Inductive Coupled Plasma Optical Emission Spectrometer) to determine the compositions of the samples taken at different reaction times. In these samples, Cu and In are presumably homogenously distributed into the host nanocrystals during the synthesis process. As shown in Table 1, four purified samples taken at different reaction times at D-concentration of 10% show similar In/Cd and Cu/Cd ratios, which means that the real Cu and In concentration in the CdS host was not changed by the growth of the CdS QDs. This results are also observed in the reactions of higher (20%, 45%) or lower dopant (6.5%) concentrations (Table S1†), which indirectly proves that the Cu and In and the Cd react with sulfide simultaneously and that process leads to the Cu and In ions being evenly incorporated into the lattice structure of CdS. Otherwise, the formation of $CuInS_2$/CdS core/shell structure or hetero-structures would result in a very sharp evolution of In/Cd and Cu/Cd ratios due to the separate formation process of $CuInS_2$ and CdS. The samples taken from the reaction at D-concentration of 2.5% show a slow evolution of In/Cd and Cu/Cd ratios with reaction time, which is most likely attributed to the formation of gradient doping nanocrystals. The Cu/In ratio of CuIn-doped CdS QDs was not the expected value of 1,[43] possibly because the different reactivities of Cu and In resulted in different chemical yields in this doping reaction or because of measurement errors (different sensitivities of Cu and In).

Table 1 The evolution of the M/Cd molar ratio in dope CdS QDs (D-concentration 10%) with increasing reaction time (M = Cu, In)

Molar ratio (M/Cd)	10 min	20 min	30 min	50 min
Cu/Cd	0.09	0.07	0.08	0.08
In/Cd	0.07	0.04	0.05	0.04

Self-reabsorption experiments

As previously mentioned, CuIn-doped CdS QDs exhibit a large Stokes shift, which is helpful to avoid the self-reabsorption of QDs, particularly in cases of high QD packing density or loading fraction. To evaluate the self-reabsorption of CuIn-doped CdS QDs, we compared their concentration quench behaviors with that of CdSe, CdSe/CdS, $CuInS_2$, and $CuInS_2$/ZnS QDs, where the concentration of the QDs was controlled by increasing the optical density (OD) at 450 nm (the emission wavelength of blue LED chips). As shown in Fig. 6, the PL intensity of CuIn-doped CdS QDs linearly increased with increasing OD until the OD was 1 and continued to increase nonlinearly until the OD was 2.2; however, the CdSe-core QDs began to exhibit concentration quenching behavior when the OD was just 0.5, and their PL intensity decreased when the OD was just 0.75. The concentration quenching behavior of $CuInS_2$ is better than that of CdSe QDs but worse than that of CuIn-doped CdS because $CuInS_2$ exhibits a Stokes shift relatively larger than that of CdSe but smaller than that of CuIn-doped CdS, as shown in Fig. 6. In addition, the concentration quench behavior of $CuInS_2$/ZnS was similar to CdSe/CdS QDs which the PL intensity decreased when OD was approximately 0.6.

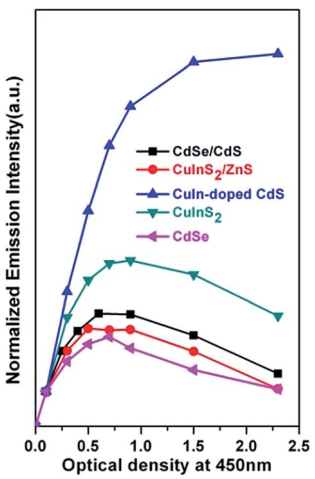

Fig. 6 Concentration quenching behaviors of different QDs.

The main reason for the concentration quenching of QDs is their self-reabsorption,[14] which is important for their potential application as red phosphors in white-light-emitting down-conversion devices that rely on a combination of a blue LED chip with coated green and red emitters. Fig. S4(a–c)† show the differences in Stokes shifts among four types of QDs. The PL emission and absorption spectra of the CuIn-doped CdS QDs have almost no overlap; on the contrary, the overlap of the CdSe QDs' absorption and emission spectra is substantial, and the overlap is almost no change when coated with three monolayers of CdS which introduces two downsides: CdSe or CdSe/CdS QDs will not only absorb green light emitted from green phosphors but will also absorb the light emitted from smaller CdSe or CdSe/CdS QDs with bluer emissions. The overlap of $CuInS_2$ QDs is little better than CdSe QDs, but with coating 3 monolayers of ZnS, such an overlap becomes more evident because of the emission spectrum's blue shift than absorption spectrum. As a result, when QDs are exposed to blue light radiation, the number of photons produced by the CuIn-doped CdS QDs will be higher than that produced by other four QDs because of the negligible reabsorption of CuIn-doped CdS QDs if their QYs are the same, consistent with the results shown in Fig. 6. If we further consider the effects of absorption of green light in white-light-emitting devices, the light output by CuIn-doped QDs will be superior to that by CdSe or CdSe/CdS QDs. The small Stokes shift of CdSe or CdSe/CdS QDs has been described as the "most fundamental concern about QDs"[14] because this feature results in self-reabsorption, which "red shifts and reduces the efficiency of light emission."[7]

Thermal quenching experiments

The thermal quenching of QD luminescence is also important for their application in functional devices, such as LED which may require thermal stable luminescence. Particularly when LED is using in display which requires phosphors with sustained brightness and high color purity at temperature frequently exceeding 100 °C.[57,58] Hence, temperature-dependent luminescence of CuIn-doped CdS QDs was tested in the range of 20–150 °C. We heated the sample (10% doping, solid film) with the highest QY from 20 °C to 150 °C while measuring the PL intensity at the given temperature. As shown in Fig. 7, similar to the cases of other QDs, the intensity of the CuIn-doped CdS QDs decreased with increasing temperature because the nonradioactive transition from the excited states to the ground state increased, this result is defined as the thermal quenching effect. They lost approximately 20% of their emission QY when heated to 150 °C, thereby exhibiting superior performance compared with that of CdSe and comparable to that of Cu:CdS/CdS.[37] We repeated this thermal quenching experiment for several cycles and observed almost no difference, which indicates the quenching behavior of CuIn-doped CdS QDs is reversible in this temperature range. Such excellent thermal stability and reversibility could make CuIn-doped CdS QDs a promising emitter for use in several applications.

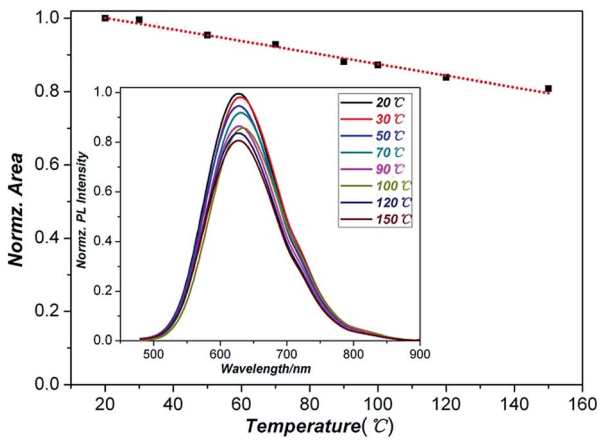

Fig. 7 Thermal quenching behavior of CuIn-doped CdS QDs (D-concentration 10%).

Experimental

Materials

1-Octadecene (ODE, 90%, GC), 1-dodecanethiol (DDT, 98%), *n*-butylamine (99%, GC), and cuprous iodide (CuI, 99.95% metals basis) were purchased from Aladdin. Indium acetate ($In(Ac)_3$, 99.99%) was purchased from Alfa Aesar. Cadmium oxide (CdO, powder, 99.5% trace metals basis) and oleic acid (OA, 90%) were purchased from Aldrich. All of the chemicals were used without further purification.

Preparation of $Cd(OA)_2$ stock solution

A $Cd(OA)_2$ stock solution (0.5 M) was prepared as follows: CdO (19.05 g) was mixed in ODE (125 mL) with oleic acid (125 mL). The mixture was heated to 120 °C under vacuum and magnetic stirring for 1 h; the mixture was subsequently backfilled with nitrogen, heated to 250 °C and refluxed until the solution became clear. The solution was then cooled to room temperature as a cadmium stock solution (0.5 M).

One-pot synthesis of CuIn-doped CdS QDs with different dopant concentrations

In a typical synthesis of doped CdS QDs, 1 mL of the $Cd(OA)_2$ precursor (0.5 mmol), 1 mL of DDT (~4 mmol) and 48 mL of ODE were mixed with 0.0125 mmol of CuI and 0.0125 mmol of $In(Ac)_3$ in a 100 mL three-neck flask under an inert atmosphere. The mixture was heated to 120 °C under a primary vacuum and magnetic stirring for 0.5 h, backfilled with N_2, and then heated to the reaction temperature of 250 °C at a rate of 13 °C min^{-1}. Aliquots were taken from the reaction solution at different intervals. Fluorescence emission and UV-vis absorption spectra of the aliquots diluted with toluene were determined to monitor the growth of quantum dot. The effect of D-concentration was studied using the same procedure previously described except a different amount of the Cu and In precursors were added to the reaction solution to achieve Cu(In)/Cd atomic ratios of 2.5%, 6.5%, 10%, 20%, and 45%.

Characterization

Transmission electron microscopy (TEM) images were taken on a JEM-2100 transmission electron microscope operated at an acceleration voltage of 200 kV. X-ray powder diffraction (XRD) patterns were obtained using a D/max-2200/PC X-ray diffractometer produced by Japan Rigaku Corporation. UV-vis spectra were recorded on a T-6 UV-visible spectrophotometer. PL spectra were recorded using Hitachi F-4500 and Ocean Optics 2000 spectrofluorometers. The valence states and amounts of the metals in the QDs were measured using an AXIS ULTRA DLD X-ray photoelectron spectrometer (XPS) and Varian 700-ES Inductively Couple Plasma Optical Emission Spectroscopy (ICP-OES), respectively.

Conclusions

In conclusion, we have successfully synthesized Cu and In co-doped CdS QDs using a single-step non-injection method. Using a strategy of co-doping with In, we easily overcame the difficulty of incorporating Cu ions into CdS QDs, and Cu^{+} ions were homogeneously doped into the CdS QDs. The emissions of these doped CdS QDs were tunable from the green to the near-infrared regions; they also exhibited a QY as high as 40% and surprisingly large Stokes shifts. We demonstrated that their Stokes shift can be tuned from 100 nm to 300 nm by tuning the dopant concentration of Cu and In and the reaction time. The extremely large Stokes shifts dramatically decreased the self-absorption of the QDs, which could be helpful of improving efficiency of QD LED devices. The decreased self-absorption of QDs is also important for bio-imaging applications, where a greater separation of the excitation and emission wavelengths can boost the signal-to-noise ratio by minimizing the noise from the excited source. Furthermore, our strategy of co-doping may be a universal way to dope group-I or -III ions into group II–IV QDs, which not only corrects the charge imbalance caused by single doping of group-I or -III ions but also enhances the solubility of the dopant ions in the host because of decreased lattice mismatch. In an initial experiment, we successfully synthesized CuIn co-doped CdSe QDs with a tunable emission beyond 1000 nm.

Acknowledgements

This work is financially supported by the National Natural Science Foundation of China (NSFC 21271179), the Program for New Century Excellent Talents (NCET-13-0364) and the State Key Program of National Natural Science Foundation of China (NSFC 21436007). We thank Professor C. Q. Dong for assistance with the PL-lifetime measurements.

Notes and references

1 S. Chakrabarti, M. A. Holub, P. Bhattacharya, T. D. Mishima, M. B. Santos, M. B. Johnson and D. A. Blom, *Nano Lett.*, 2005, **5**, 209.
2 H. V. Demir, U. O. S. Seker, G. Zengin, E. Mutlugun, E. Sari, C. Tamerler and M. Sarikaya, *ACS Nano*, 2011, **5**, 2735.
3 Q. Sun, Y. A. Wang, L. S. Li, D. Wang, T. Zhu, J. Xu, C. Yang and Y. Li, *Nat. Photonics*, 2007, **1**, 717.
4 P. O. Anikeeva, J. E. Halpert, M. G. Bawendi and V. Bulovic, *Nano Lett.*, 2009, **9**, 2532.
5 J. Zhao, J. A. Bardecker, A. M. Munro, M. S. Liu, Y. Niu, I.-K. Ding, J. Luo, B. Chen, A. K. Y. Jen and D. S. Ginger, *Nano Lett.*, 2006, **6**, 463.
6 S. Jun, J. Lee and E. Jang, *ACS Nano*, 2013, **7**, 1472.
7 J. M. Phillips, M. E. Coltrin, M. H. Crawford, A. J. Fischer, M. R. Krames, M. R. Mueller, G. O. Mueller, Y. Ohno, L. E. Rohwer and J. A. Simmons, *Laser Photonics Rev.*, 2007, **1**, 307.
8 H. S. Jang, H. Yang, S. W. Kim, J. Y. Han, S. G. Lee and D. Y. Jeon, *Adv. Mater.*, 2008, **20**, 2696.
9 E. Jang, S. Jun, H. Jang, J. Lim, B. Kim and Y. Kim, *Adv. Mater.*, 2010, **22**, 3076.
10 Y. Li, A. Rizzo, R. Cingolani and G. Gigli, *Microchim. Acta*, 2007, **159**, 207.
11 M. J. Panzer, V. Wood, S. M. Geyer, M. G. Bawendi and V. Bulović, *J. Disp. Technol.*, 2010, **6**, 90.
12 J. Lim, S. Jun, E. Jang, H. Baik, H. Kim and J. Cho, *Adv. Mater.*, 2007, **19**, 1927.
13 W. Chung, K. Park, H. J. Yu, J. Kim, B.-H. Chun and S. H. Kim, *Opt. Mater.*, 2010, **32**, 515.
14 J. Kundu, Y. Ghosh, A. M. Dennis, H. Htoon and J. A. Hollingsworth, *Nano Lett.*, 2012, **12**, 3031.
15 P. F. Smet, A. B. Parmentier and D. Poelman, *J. Electrochem. Soc.*, 2011, **158**, 37.
16 T. Xuan, S. Wang, X. Wang, J. Liu, J. Chen, H. Li, L. Pan and Z. Sun, *Chem. Commun.*, 2013, **49**, 9045.
17 T. Yao, S. Kou, Y. Sun, Q. Zhao and J. Yang, *CrystEngComm*, 2012, **14**, 8440.
18 V. K. Sharma, B. Guzelturk, T. Erdem, Y. Kelestemur and H. V. Demir, *ACS Appl. Mater. Interfaces*, 2014, **6**, 3654.
19 R. Viswanatha, S. Sapra and S. Sen Gupt, *J. Phys. Chem. B*, 2004, **108**, 6303.
20 N. Pradhan, D. Goorskey, J. Thessing and X. G. Peng, *J. Am. Chem. Soc.*, 2005, **127**, 17586.
21 R. Lozada-Morales, O. Portillo-Moreno, S. A. Tomás and O. Zelaya-Angel, *Opt. Mater.*, 2013, **35**, 1023.
22 Z. Huang, X. Zou and H. Zhou, *Mater. Lett.*, 2013, **95**, 139.
23 S. Gul, J. K. Cooper, P.-A. Glans, J. Guo, V. K. Yachandra, J. Yano and J. Z. Zhang, *ACS Nano*, 2013, **7**, 8680.
24 S. Brovelli, C. Galland, R. Viswanatha and V. I. Klimov, *Nano Lett.*, 2012, **12**, 4372.
25 M. J. Rao, T. Shibata, S. Chattopadhyay and A. Nag, *J. Phys. Chem. Lett.*, 2013, **5**, 167.
26 R. Fu, N. Yoshizawa, M. S. Dresselhaus, G. Dresselhaus, J. H. Satcher and T. F. Baumann, *Langmuir*, 2002, **18**, 10100.
27 H. Ye, A. Tang, L. Huang, Y. Wang, C. Yang, Y. Hou, H. Peng, F. Zhang and F. Teng, *Langmuir*, 2013, **29**, 8728.
28 S. Zhang, F. Hu, J. He, W. Cheng, Q. Liu, Y. Jiang, Z. Pan, W. Yan, Z. Sun and S. Wei, *J. Phys. Chem. C*, 2013, **117**, 24913.
29 S. Shen, L. Zhao, Z. Zhou and L. Guo, *J. Phys. Chem. C*, 2008, **112**, 16148.

30 D. H. Xu and W. Z. Shen, *J. Phys. Chem. C*, 2012, **116**, 13368.
31 A. La Rosa-Toro, R. Berenguer, C. Quijada, F. Montilla, E. Morallon and J. Vazquez, *J. Phys. Chem. B*, 2006, **110**, 24021.
32 R. Xie and X. G. Peng, *J. Am. Chem. Soc.*, 2009, **131**, 10645.
33 A. Tang, L. Yi, W. Han, F. Teng, Y. Wang, Y. Hou and M. Gao, *Appl. Phys. Lett.*, 2010, **97**, 033112.
34 R. Viswanatha, S. Chakraborty, S. Basu and D. Sarma, *J. Phys. Chem. B*, 2006, **110**, 22310.
35 B. B. Srivastava, S. Jana and N. Pradhan, *J. Am. Chem. Soc.*, 2010, **133**, 1007.
36 A. Pandey, S. Brovelli, R. Viswanatha, L. Li, J. Pietryga, V. I. Klimov and S. Crooker, *Nat. Nanotechnol.*, 2012, **7**, 792.
37 G. K. Grandhi and R. Viswanatha, *J. Phys. Chem. Lett.*, 2013, **4**, 409.
38 K. Era, S. Shionoya and Y. Washizawa, *J. Phys. Chem. Solids*, 1968, **29**, 1827.
39 K. Era, S. Shionoya, Y. Wasfflzawa and H. Ohmatsu, *J. Phys. Chem. Solids*, 1968, **29**, 1843.
40 T. Kryshtab, V. Khomchenko, V. Papusha, M. Mazin and Y. A. Tzyrkunov, *Thin Solid Films*, 2002, **403**, 76.
41 M. Aven and J. Parodi, *J. Phys. Chem. Solids*, 1960, **13**, 56.
42 Y. Chen, J. Duh, B. Chiou and C. Peng, *Thin Solid Films*, 2001, **392**, 50.
43 L. Li, A. Pandey, D. J. Werder, B. P. Khanal, J. M. Pietryga and V. I. Klimov, *J. Am. Chem. Soc.*, 2011, **133**, 1176.
44 L. Li, T. J. Daou, I. Texier, T. T. Kim Chi, N. Q. Liem and P. Reiss, *Chem. Mater.*, 2009, **21**, 2422.
45 L. Manna, *Chem. Mater.*, 2012, **24**, 2400.
46 R. Xie, M. Rutherford and X. G. Peng, *J. Am. Chem. Soc.*, 2009, **131**, 5691.
47 W. S. Song and H. Yang, *Chem. Mater.*, 2012, **24**, 1961.
48 G. A. Crosby and J. N. Demas, *J. Phys. Chem.*, 1971, **75**, 991.
49 I. Robel, M. Kuno and P. V. Kamat, *J. Am. Chem. Soc.*, 2007, **129**, 4136.
50 K. Konishi and T. Hiratani, *Angew. Chem., Int. Ed.*, 2006, **45**, 5191.
51 A. V. Isarov and J. Chrysochoos, *Langmuir*, 1997, **13**, 3142.
52 S. Jana, B. B. Srivastava, S. Acharya, P. K. Santra, N. R. Jana, D. Sarma and N. Pradhan, *Chem. Commun.*, 2010, **46**, 2853.
53 J. Suyver, T. Van der Beek, S. Wuister, J. Kelly and A. Meijerink, *Appl. Phys. Lett.*, 2001, **79**, 4222.
54 X. Li, H. Shen, S. Li, J. Z. Niu, H. Wang and L. S. Li, *J. Mater. Chem.*, 2010, **20**, 923.
55 K. H. Park, Y. W. Lee, D. Kim, K. Lee, S. B. Lee and S. W. Han, *Chem.–Eur. J.*, 2012, **18**, 5874.
56 J. F. Moulder, W. F. Stickle, P. E. Sobol and K. D. Bomben, *Handbook of X-Ray Photoelectron Spectroscopy*, Perkin-Elmer, Boca Raton, FL, 1992.
57 B. T. Diroll and C. B. Murray, *ACS Nano*, 2014, **8**, 6466.
58 C. E. Rowland, W. Y. Liu, D. C. Hannah, M. K. Y. Chan, D. V. Talapin and R. D. Schaller, *ACS Nano*, 2013, **8**, 977.